metals

MDPI

Article

Ruta graveolens Plant Extract as a Green Corrosion Inhibitor for 304 SS in 1 M HCl: Experimental and Theoretical Studies

Sonia Estefanía Hernández-Sánchez [1], Juan Pablo Flores-De los Rios [2], Humberto Alejandro Monreal-Romero [3], Norma Rosario Flores-Holguin [4], Luz María Rodríguez-Valdez [5], Mario Sánchez-Carrillo [2], Anabel D. Delgado [6] and Jose G. Chacón-Nava [1,*]

1 Department of Mellurgy and Structural Integrity, Advanced Materials Research Center (CIMAV), Miguel de Cervantes 120, Complejo Industrial Chihuahua, Chihuahua 31136, Chih., Mexico; sonia.hernandez@cimav.edu.mx
2 Department Metal-Mechanical, Tecnológico Nacional de México-Instituto Tecnológico de Chihuahua, Av. Tecnológico 2909, Chihuahua 31130, Chih., Mexico; juan.fd@chihuahua.tecnm.mx (J.P.F.-D.l.R.); mario.sc@chihuahua.tecnm.mx (M.S.-C.)
3 Department of Biomaterials Science and Nanotechnology, University of Chihuahua (UACH), Chihuahua 31000, Chih., Mexico; hmonreal@uach.mx
4 NANOCOSMOS Virtual Laboratory, Department of Environment and Energy, Advanced Materials Research Center (CIMAV), Miguel de Cervantes 120, Complejo Industrial Chihuahua, Chihuahua 31136, Chih., Mexico; norma.flores@cimav.edu.mx
5 Faculty of Chemical Sciences, Autonomous University of Chihuahua (UACH), Chihuahua 31125, Chih., Mexico; lmrodrig@uach.mx
6 Department of Engineering and Materials Chemistry, Advanced Materials Research Center (CIMAV), Miguel de Cervantes 120, Complejo Industrial Chihuahua, Chihuahua 31136, Chih., Mexico; anabel.delacruz@cimav.edu.mx
* Correspondence: jose.chacon@cimav.edu.mx

Abstract: This study evaluated the corrosion inhibitory effects of *Ruta graveolens* leaf extract for 304 stainless steel in 1 M HCl. The analysis of the leaf extract using HPLC indicated that the primary compounds present in the leaf extract were rutin, caffeic acid, p-coumaric acid, and apigenin. The inhibition efficiency (*IE*%) of the extract was studied using weight loss, potentiodynamic polarization, electrochemical impedance spectroscopy (EIS), and computational simulation (density functional theory, DFT). The effects of the inhibitor concentration and solution temperature were investigated. The results indicated that the *IE*% increased for increasing concentrations of the extract, while the reverse was true with increasing temperatures. At 25 °C and a 600 ppm extract concentration, the results indicated a maximum inhibition efficiency of 95%, 98%, and 96% by weight loss, potentiodynamic polarization, and EIS techniques, respectively. SEM observations showed a significant change in the surface morphology of the 304 SS with and without the addition of the inhibitor compound. At all temperatures, the adsorption of the inhibitor components onto the 304 SS surface was found to follow the Langmuir isotherm model, and the inhibition process was governed by physical adsorption. Furthermore, chemical interactions between the inhibitor and the 304 SS steel surface were elucidated via density functional theory (DFT) calculations.

Keywords: green corrosion inhibitor; *Ruta graveolens* extract; 304 SS; PDP; EIS; DFT

Citation: Hernández-Sánchez, S.E.; Flores-De los Rios, J.P.; Monreal-Romero, H.A.; Flores-Holguin, N.R.; Rodríguez-Valdez, L.M.; Sánchez-Carrillo, M.; Delgado, A.D.; Chacón-Nava, J.G. *Ruta graveolens* Plant Extract as a Green Corrosion Inhibitor for 304 SS in 1 M HCl: Experimental and Theoretical Studies. *Metals* **2024**, *14*, 1267. https://doi.org/10.3390/met14111267

Academic Editor: Changdong Gu

Received: 1 October 2024
Revised: 26 October 2024
Accepted: 2 November 2024
Published: 8 November 2024

1. Introduction

It is well known that stainless steel is corrosion resistant due to the thin passive film that forms on its surface. An essential property of this passive film is that it can spontaneously self-repair when damaged. As a result, stainless steels are widely used in corrosive environments and many industrial applications. However, in the presence of chlorides or other aggressive anions, they are prone to localized corrosion [1,2].

Among the different protection methods, in recent years, green corrosion inhibitors have been gaining preference over inhibitors of inorganic origin due to their lower cost,

availability, and low toxicity. Adding relatively small amounts of inhibitor to the aggressive environment has given good results in slowing down the corrosion rate [3,4]. It has been reported that the adsorption of an inhibitor on a metal surface is highly dependent on the electrostatic interaction, the mode of adsorption, the structure of the molecule, and the solution or electrolyte employed [5]. The adsorption properties of inhibitors of organic origin depend mainly on some physicochemical properties of the molecules, the functional groups, the possible steric effects, the electron density of the donor atoms, and the potential interaction of the p orbitals of the inhibitor with the d orbitals of the atoms of the metal surface. These properties establish a degree of adsorption of the inhibitor molecules on the solid surface, resulting in a corrosion protection barrier [6].

Green inhibitor compounds are usually produced from plants' natural extracts, such as their leaves, stems, and roots, and organic wastes, such as eggshells, apples, oranges, walnuts, shrimp, etc. These extracts can adsorb on the metal surface physically or chemically, providing a better corrosion inhibition resource. This behavior is due to flavonoids and phenolic acids that can interact with the metal surface by donating a lone pair of electrons from heteroatom and unsaturated aromatic systems [7]. The development of green corrosion inhibitors is booming due to the increasing popularity of green chemistry in science and technology. In recent decades, using plant extracts as corrosion inhibitors has brought significant attention due to their lower environmental risk, lower cost, wide availability, and high inhibition effectiveness. Therefore, these materials are suitable candidates to replace traditional synthetic corrosion inhibitors, which are expensive and toxic. The use of natural products as corrosion inhibitors dates back to 1930 when plant extracts of Celidonia (Chelidonium majus) and other plants were first used in H_2SO_4 pickling. After that, the interest in using natural products as corrosion inhibitors increased substantially. Undoubtedly, the development and application of green inhibitors has been focused on carbon steels. Regarding this, over the last four years, reports from the literature mention the use of compounds such as *Lilium brownii* leaves [8], *Rhynchostylis retusa* [9], *Ammi visnaga* L. extract [10], *Betel* leaves [11], *Mandevilla fragans* leaves [12], *Ustilago maydis* extract [13], *Cape gooseberry* extract [14], Thevetia peruvuana extract [15], Saussurea obvallatta extract [16], Laurus tamala leaves [17], and Tabebuia heterophylla leaves [18]. In the last decade, the development of alternative green corrosion inhibitors for austenitic stainless steels has been studied: E.A Fouda et al. [19] reported using Calotropis procera extract as a corrosion inhibitor for a 304 austenitic stainless steel, obtaining a maximum efficiency of 75.3%. Ehsani et al. [20] reported that using Thymus vulgaris extract obtained a maximum inhibition efficiency of 62%. Albrimi et al. [21] studied the effect of Heptamolybdate ions as an inhibitor and reported that the corrosion rate in an acidic medium was considerably reduced, obtaining an efficiency of 91.2%. Fouda et al. [22] studied the effect of Chalcones (aromatic ketones) on the corrosion behavior of type 304 stainless steel in a HCl solution, showing that the inhibitor efficiency increased with an increasing concentration and decreased with an increasing temperature, reporting a maximum inhibition efficiency of 88%. Soltani et al. [23] studied the effect of Silybum marianum leaf extract as a corrosion inhibitor for a 304 stainless steel in an acidic medium (1 M HCl), employing weight loss measurements, potentiodynamic polarization, and electrochemical impedance spectroscopy techniques, reporting that this extract behaved as a mixed-type inhibitor, giving a maximum efficiency of 98%. Scendo et al. [24] studied the influence of Adenine on the corrosion of 304 SS in chloride-containing solutions. The Tafel polarization technique revealed that the inhibitor is a mixed-type inhibitor and indicated that the efficiency increases with an increasing Adenine concentration and temperature, obtaining a maximum efficiency of 94%. Soltani et al. [25] studied the inhibitory effect of Salvia officinalis extract on 304 stainless steel in hydrochloric acid solution using the techniques of electrochemical impedance spectroscopy, polarization curves, and weight loss measurements. The results indicated that the inhibitor is of a mixed type, and the maximum inhibition efficiency reported was 96.2%. Despite the variety of reports on using plant extracts as green inhibitors on metals in acidic solutions, there is still a need to investigate other plants with potential use as corrosion inhibitors

in industrial applications. *Ruta graveolens* is an aromatic plant belonging to the Rutaceae family and finds frequent use in medicinal applications [26]. Regarding metallic corrosion problems, few studies on carbon steel exposed to acidic media have reported using *Ruta graveolens* extract as a corrosion inhibitor, with the results showing a favorable effect in decreasing the corrosion rate [27,28]. To our knowledge, there are no reports on the inhibitory effect of this plant applied on stainless steels in an acidic medium. Therefore, the present study examines *Ruta graveolens* extract as a corrosion inhibitor on 304 stainless steel exposed to a 1 M HCl solution. Weight loss measurements, potentiodynamic polarization (PDP), and electrochemical impedance spectroscopy (EIS) techniques were employed to evaluate the effects of extract concentration and temperature on the corrosion rate. In addition, quantum chemical calculations using density functional theory (DFT) elucidated the chemical interactions between the inhibitor and the 304 stainless steel surface. Thus, this extract's good inhibitory behavior in acidic media may find potential uses in the petrochemical industry and industrial processes, such as acid pickling and acid descaling in heat exchangers, condensers, etc. [29].

2. Materials and Methods

2.1. Materials

An austenitic stainless steel of type 304 with the following chemical composition was used as a test material, see Table 1:

Table 1. Chemical composition (wt %) of the 304 stainless steel used.

C	Cr	Ni	Mn	Si	P	S	Fe
0.07	18.18	8.48	2.01	0.75	0.045	0.03	Bal.

The dimensions of the experimental specimens were as follows: 1.25 cm in diameter and 1 cm in length. Then, all the specimens for the electrochemical tests were encapsulated with epoxy resin, leaving an exposed area of 1.27 cm^2 for the electrochemical tests. For the weight loss tests, the specimens were not encapsulated. All specimens were sanded with silicon carbide paper to grade 600 and ultrasonically cleaned with ethanol.

The corrosive medium was a 1 M HCl solution prepared using 37% analytical-grade hydrochloric acid (J.T. Baker) and distilled water. The concentrations of *Ruta graveolens* extract were 150, 300, 450, and 600 ppm, and HCl solution without an added inhibitor was used as a blank.

2.2. Extract Preparation

Ten grams of dried *Ruta graveolens* leaves were weighed and placed into a Soxhlet extraction apparatus. A total of 250 mL of absolute ethyl alcohol (J.T. Baker) was used as a solvent and placed inside a round bottom flask. An electric heater was used to heat the solvent and reflux the mixture. A recirculation bath maintained the condenser of the extraction apparatus at 8 °C to prevent solvent leakage. After 8 h of operation, the ethanolic extract of *R. graveolens* was placed under refrigeration at 4 °C for further analysis.

2.3. Characterization of Ruta Graveolens Extract

The extract was characterized using high-performance liquid chromatography (HPLC) using a Thermo DIONEX Ultimate 3000 liquid chromatograph (Thermo Fisher Scientific Inc., Waltham, MA, USA). The separation was carried out on a 250 mm × 4.6 mm Quasar C18 column (Perkin Elmer, Waltham, MA, USA). with a particle size of 5 µm. The mobile phase consisted of 0.1% water and sulfuric acid (line A) or acetonitrile (line B). The gradient was as follows: 90%A/10%B, 0–12 min; 70%A/30%B, 12–14 min; 60%A/40%B, 14–18 min; 50%A/50%B, 18–20 min; 20%A/80%B, 20–24 min; 10%A/90%B, 24–28 min; and 0%A/100%B, 28–30 min. The injection volume was 20 µL, and the wavelength was 270 nm. Peaks were identified by comparing the retention times of the standards ana-

lyzed under the same conditions. Sigma-Aldrich supplied the analytical-grade phenolic compound standards.

2.4. Weight Loss Measurement

The weight loss method for monitoring the corrosion rate and inhibition efficiency is helpful because of its simple application and reliability. The inhibition efficiency of *Ruta graveolens* leaves was calculated for 304 austenitic stainless steel. For each test condition, three samples were immersed in 1 M HCl, with and without extract. The following equation was used to measure the corrosion rate and extract efficiency by varying the concentration of the extract:

$$C_R = \frac{\mathrm{KW}}{\mathrm{At}\rho} \quad (1)$$

where the corrosion rate, C_R, is calculated in mm/year, W is the weight loss, t is the immersion time, ρ is the density of 304 SS steel (8.0 g/cm^3), and K is the corrosion constant $\left(8.76 \times 10^4\right)$. The inhibition efficiency *IE*% was based on the weight loss measured over the exposure times of each test and was calculated using the following equation:

$$IE = \left(\frac{W^0 - W}{W^0}\right) \times 100 \quad (2)$$

W^o and W are the weight loss of the specimens in the corrosive media without inhibitor and solutions with inhibitor, respectively. In general, it is accepted to assume that the inhibitor efficiency is due to a blocking effect of the adsorbed species. Thus, the value of the surface degree covered equals $\Theta = IE\% \times (100)^{-1}$ [30].

The samples were weighed for an initial mass recording using a Sartorius Mod MC 210S analytical balance (Sartorius AG, Gottingen, Germany)) with a resolution of 0.00001 g. Subsequently, they were exposed to a corrosive 1 M HCl medium without inhibitor (blank solution), and then, concentrations of 150, 300, 450, and 600 ppm of .*Ruta graveolens* extract were added. The exposure times were 2, 4, 6, and 8 h at three temperatures: 25 °C, 40 °C, and 60 °C. After the corresponding immersion time, the specimens were cleaned according to ASTM G1 [31] and reweighed for final weight recording.

2.5. Electrochemical Measurements

For the electrochemical tests, a jacketed glass cell was used with a conventional three-electrode arrangement consisting of 304 stainless steel as the working electrode, platinum wire as the counter electrode, and a Ag/AgCl electrode as the reference electrode. In each experiment, a volume of 150 mL of naturally aerated electrolyte solution was employed in the cell without and with the addition of an inhibitor. Before starting the measurements with potentiodynamic polarization and electrochemical impedance spectroscopy techniques, the working electrode was immersed for at least 60 min to stabilize the open-circuit potential. All experiments were performed with the test medium under static conditions at 25 °C, 40 °C, and 60 °C.

The polarization curves were obtained using a Gill AC potentiostat (ACM Instruments, Cambria, UK), and data analysis was performed with commercial Gill AC 1561 version 4.0 software. After the open-circuit potential stabilized, potentiodynamic polarization curves were obtained for the different inhibitor concentration and temperature conditions, using a sweep speed of 1 mV/s and a potential range of −300 to 500 mV relative to Ecorr. *Ruta graveolens* extract was added in the corrosive medium of 1 M HCl at concentrations of 150, 300, 450, and 600 ppm.

In this technique, *IE*% was defined as:

$$IE\% = \left(\frac{I^b_{corr} - I^{inh}_{corr}}{I^b_{corr}}\right) \times 100 \quad (3)$$

where I_{corr}^{b} and I_{corr}^{inh} are the corrosion current density values without and with inhibitor, respectively.

Impedance tests were performed on a workstation with an AUTOLAB potentiostat. Impedance measurements (Metrohm, Herisau, Switzerland) were performed at open-circuit potential over a frequency range of 100 KHz to 0.01 Hz with an AC signal amplitude perturbation of ±10 mV.

In this case, the percentage efficiency was calculated from the R_{ct} values using the following equation:

$$\%E = \frac{R_{ct} - R_{ct}^{0}}{R_{ct}} \times 100 \quad (4)$$

where R_{ct}^{0} and R_{ct} are the charge-transfer resistance in the absence and presence of *R. graveolens* extract, respectively.

2.6. Quantum Chemical Calculations

DFT methods for corrosion inhibition studies are very important for predicting which adsorption mechanism occurs at the metal–inhibitor molecule interface. These calculations were performed using the Gaussian 9.0 program and Gauss View 5.0 visualizer (Gaussian Inc., Wallingford, CT, USA) [32]. Theoretical quantum calculations of phenolic acids in *Ruta graveolens* extract were performed using density functional theory (DFT). The optimization of the ground state geometry and frequency calculations were performed using the hybrid density functional B3LYP [33–35] and the meta-GGA functionals M06 and M06-2X [36]. All functionals were combined with the 6-311G (d,p) basis set. The optimized geometries were used to perform the frequency calculations for each compound and verify the minimum potential energy. The absence of imaginary frequencies confirmed the minimum energy of the structure. From the optimized molecules, the HOMO, LUMO, and energy gap energies were calculated. The calculated geometry of the molecules was compared with the experimental X-ray diffraction data reported in the literature to find the optimal methodology for the reactivity calculations.

Once the methodology was defined, other theoretical properties that were also determined are the energies of the molecules in their neutral (EN), anionic (E_{N+1}), and cationic (E_{N-1}) forms, calculated using the B3LYP/6-311G (d,p) methodology. The computed energies were used to perform global reactivity calculations: ionization potential (I), electron affinity (EA), electronegativity (χ), and hardness (η). The equations for the above-mentioned molecular properties are shown below. These calculated molecular properties were applied to determine the fraction of transferred electrons (ΔN), which describes the fractional number of electrons transferred from system A (phenolic acids or flavonoids) to system B (metal surface) (see Equation (9)). All these molecular properties were calculated in the solvent phase using ethanol and the IRC solvation method.

$$I = E_{N-1} - E_N \quad (5)$$

$$EA = E_N - E_{N+1} \quad (6)$$

$$\chi = \frac{I + EA}{2} \quad (7)$$

$$\eta = \frac{I - EA}{2} \quad (8)$$

$$\Delta N = \frac{\chi_b - \chi_A}{2(\eta_b + \eta_A)} \quad (9)$$

3. Results and Discussion

3.1. HPLC Analysis of Ruta Graveolens Extract

The extract's HPLC analysis results mainly indicated the compounds shown in Figure 1: phenolic acids such as caffeic acid and p-coumaric acid and the presence of two flavonoids, rutin and apigenin.

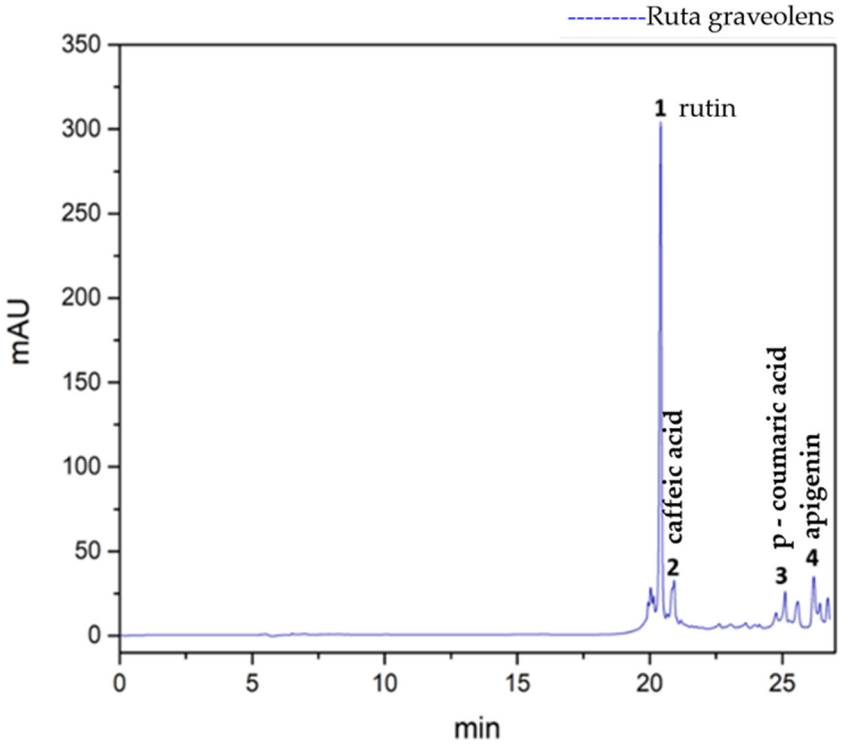

Figure 1. Chromatogram of *Ruta graveolens* extract showing the detected compounds: (**1**) rutin, (**2**) caffeic acid, (**3**) p-coumaric acid, and (**4**) apigenin.

3.2. Weight Loss

Table 2 shows the values of the corrosion rate, *CR*, and the percentage of inhibition efficiency, *IE*%, obtained for different concentrations of *Ruta graveolens* and temperatures in a 1 M HCl solution. The results show that increasing the concentration of *Ruta graveolens* increases the percentage efficiency, most likely due to an increase in the inhibitor's adsorption and degree of coverage (Θ) on the steel surface. In contrast, the opposite occurs with an increasing temperature and immersion time. Figures 2–4 show, in each case, the weight loss data versus the time and efficiency of the extract versus the immersion time with and without extract.

Table 2. Effects of *Ruta graveolens* extract concentration and temperature on *IE*% from weight loss measurements.

Temperature (°C)	Time (h)	Concentration (ppm)	Weight Loss (mg cm^{-2})	Standard Deviation	Corrosion Rate (mm/y)	θ	*IE*%
25	2	Blank	0.1568	0.00356	13.9870	-	-
		150	0.0148	0.00277	1.3570	0.91	91.14
		300	0.0119	0.00148	1.0946	0.92	92.34
		450	0.0072	0.00019	0.6639	0.95	95.22
		600	0.0072	0.00048	0.6570	0.95	95.28

Table 2. *Cont.*

Temperature (°C)	Time (h)	Concentration (ppm)	Weight Loss (mg cm^{-2})	Standard Deviation	Corrosion Rate (mm/y)	θ	*IE*%
	4	Blank	0.2446	0.00114	11.1122	-	-
		150	0.0224	0.00046	1.0225	0.91	91.22
		300	0.0203	0.00677	0.9287	0.92	92.14
		450	0.0199	0.00570	0.9121	0.92	92.35
		600	0.0140	0.00690	0.6409	0.94	94.58
	6	Blank	0.2857	0.00155	8.6925	-	-
		150	0.0380	0.000747	1.1578	0.86	86.02
		300	0.0361	0.000418	1.0994	0.87	87.13
		450	0.0277	0.000263	0.8445	0.9	90.05
		600	0.0223	0.00982	0.6812	0.92	92.12
	8	Blank	0.3729	0.00801	8.5089	-	-
		150	0.0578	0.00289	1.31928	0.8	80.15
		300	0.0428	0.00940	0.9774	0.85	85.87
		450	0.0431	0.00401	0.9843	0.85	85.41
		600	0.0309	0.00358	0.7062	0.89	89.32
40	2	Blank	0.2296	0.00238	20.9755	-	-
		150	0.0723	0.00427	6.6006	0.69	69.65
		300	0.0686	0.00360	6.2629	0.7	70.02
		450	0.0506	0.00947	4.6174	0.78	78.41
		600	0.0390	0.00130	3.5609	0.83	83.83
	4	Blank	0.2440	0.00233	15.8622	-	-
		150	0.0793	0.00224	3.6182	0.68	68.05
		300	0.0730	0.00217	3.3349	0.7	70.01
		450	0.0566	0.00932	2.5866	0.77	77.14
		600	0.0521	0.00837	2.3784	0.79	79.05
	6	Blank	0.3421	0.00155	10.5748	-	-
		150	0.1097	0.00536	3.3370	0.68	68.02
		300	0.1035	0.00228	3.1496	0.7	70.12
		450	0.0848	0.00146	2.5817	0.75	75.41
		600	0.0840	0.00159	2.5574	0.75	75.05
	8	Blank	0.4421	0.00111	9.9538	-	-
		150	0.1734	0.00867	3.9578	0.6	60.12
		300	0.1571	0.00246	3.5839	0.64	64.48
		450	0.1453	0.00510	3.3153	0.67	67.41
		600	0.1436	0.00563	3.2765	0.68	68.22
60	2	Blank	0.2839	0.00667	25.9144	-	-
		150	0.0869	0.00067	0.7877	0.69	69.63
		300	0.0883	0.00387	0.8009	0.69	69.72

Table 2. *Cont.*

Temperature (°C)	Time (h)	Concentration (ppm)	Weight Loss (mg cm^{-2})	Standard Deviation	Corrosion Rate (mm/y)	θ	*IE*%
		450	0.0713	0.00317	0.64633	0.75	75.15
		600	0.0561	0.00896	0.5084	0.8	80.21
	4	Blank	0.3337	0.00125	15.2289	-	-
		150	0.1118	0.00478	5.1042	0.67	67.12
		300	0.1103	0.00312	5.0334	0.67	67.81
		450	0.0962	0.00487	4.3894	0.71	71.11
		600	0.0758	0.00383	3.4611	0.77	77.41
	6	Blank	0.4142	0.00024	12.6012	-	-
		150	0.1502	0.00936	4.5703	0.64	64.01
		300	0.1365	0.00197	4.1533	0.67	67.47
		450	0.1266	0.00169	3.8527	0.69	69.61
		600	0.1172	0.00698	3.5662	0.72	72.52
	8	Blank	0.5413	0.00155	12.3486	-	-
		150	0.2267	0.00611	5.1732	0.58	58.87
		300	0.2104	0.00284	4.7998	0.61	61.09
		450	0.1897	0.00752	4.3289	0.65	65.15
		600	0.1802	0.00853	4.1125	0.67	67.25

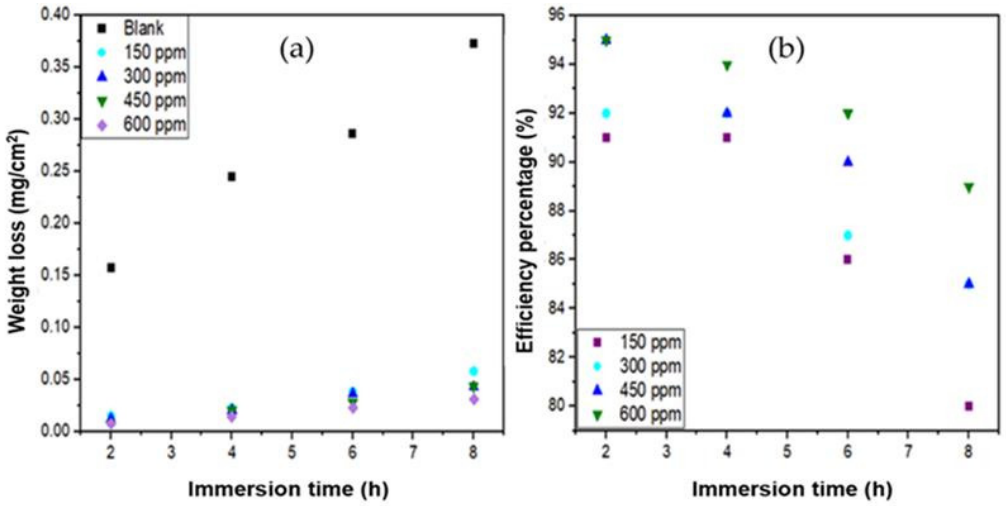

Figure 2. Plots of (**a**) weight loss vs. immersion time and (**b**) efficiency percentage vs. time for the corrosion of 304SS without and with various concentrations of *Ruta graveolens* extract in 1 M HCl at 25 °C.

The performance of *Ruta graveolens* extract at concentrations of 150, 300, 450, and 600 ppm at 25 °C is shown in Figure 2, showing (a) weight loss vs. immersion time and (b) percentage efficiency vs. immersion time. At an exposure time of 2 h, the maximum efficiency percentage value of 95.28% was obtained with 600 ppm of inhibitor. At this inhibitor concentration and 4 h of exposure, the maximum efficiency value was 94.58%. At 6 h of immersion, the maximum efficiency obtained was 92.12%. Finally, at 8 h of immersion, the maximum efficiency value was 89.32%.

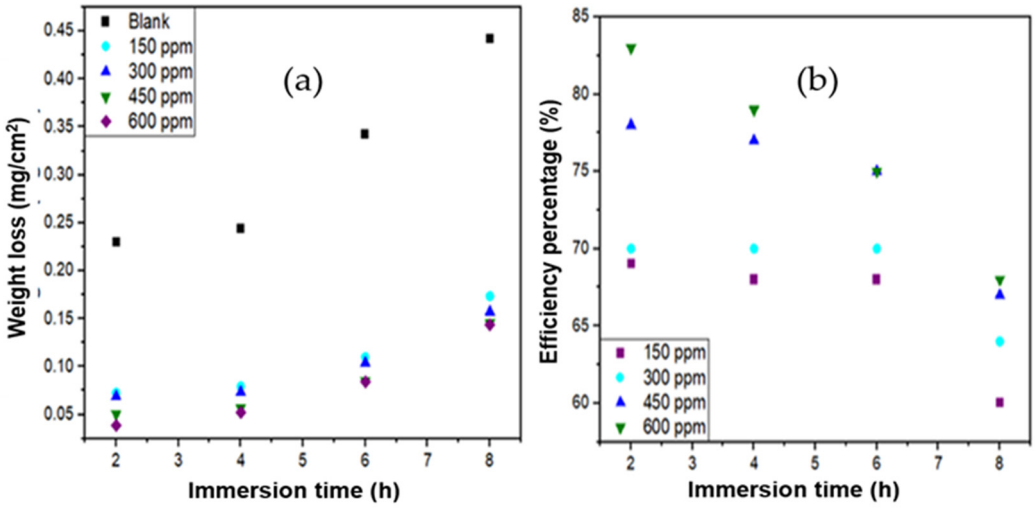

Figure 3. Plots of (**a**) weight loss vs. immersion time and (**b**) efficiency percentage vs. time for the corrosion of 304 SS without and with various concentrations of *Ruta graveolens* extract in 1 M HCl at 40 °C.

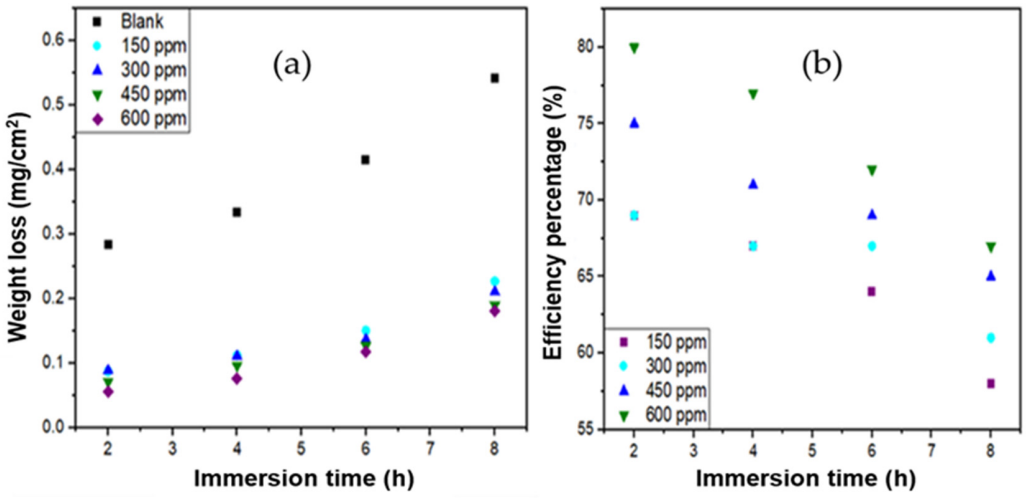

Figure 4. Plots of (**a**) weight loss vs. immersion time and (**b**) efficiency percentage vs. time for the corrosion of 304 SS without and with various concentrations of *Ruta graveolens* extract in 1 M HCl at 60 °C.

At 40 °C, the performance of the extract as a corrosion inhibitor at an exposure time of 2 h showed that the maximum efficiency achieved was 83.83% at an inhibitor concentration of 600 ppm (see Figure 3). At this concentration and 4 h of immersion, the efficiency percentage was 79.05%. After 6 h, the maximum efficiency percentage was 75.05%. At 8 h, the maximum efficiency percentage reached was 68.22%.

At 60 °C, Figure 4 shows the behavior of *Ruta graveolens* extract for different exposure times at 600 ppm. The maximum efficiency value was 80.21% at 2 h of immersion, while at 4, 6, and 8 h of immersion, the efficiencies were 77.41%, 72.52%, and 67.25%, respectively.

The experimental data obtained using the weight loss method reveal that the corrosion rate of 304 steel decreases with the addition of *Ruta graveolens* extract, obtaining the maximum inhibition efficiency at an extract concentration of 600 ppm. Conversely, with temperature and immersion time increases, the inhibition efficiency decreases.

3.3. Potentiodynamic Polarization Measurements

The effect of adding *Ruta graveolens* extract at various concentrations and temperatures on the potentiodynamic polarization curves of 304 SS steel in 1 M HCl solution is shown in Figure 5. In particular, active–passive transitions were found in all cases for the solutions with inhibitors. The values of the electrochemical parameters obtained, such as the corrosion potential (E_{corr}), current density (I_{corr}), anodic (b_a) and cathodic (b_c) Tafel slopes, and inhibition efficiency percentages ($IE\%$) obtained from the extrapolation of the Tafel curves, are given in Table 3. The results show that with an increasing inhibitor concentration, the corrosion current densities decrease independently of the temperature. Conversely, increases in the experimental temperature cause an increase in the observed corrosion current densities. Conversely, increases in the experimental temperature cause an increase in the observed corrosion current densities.

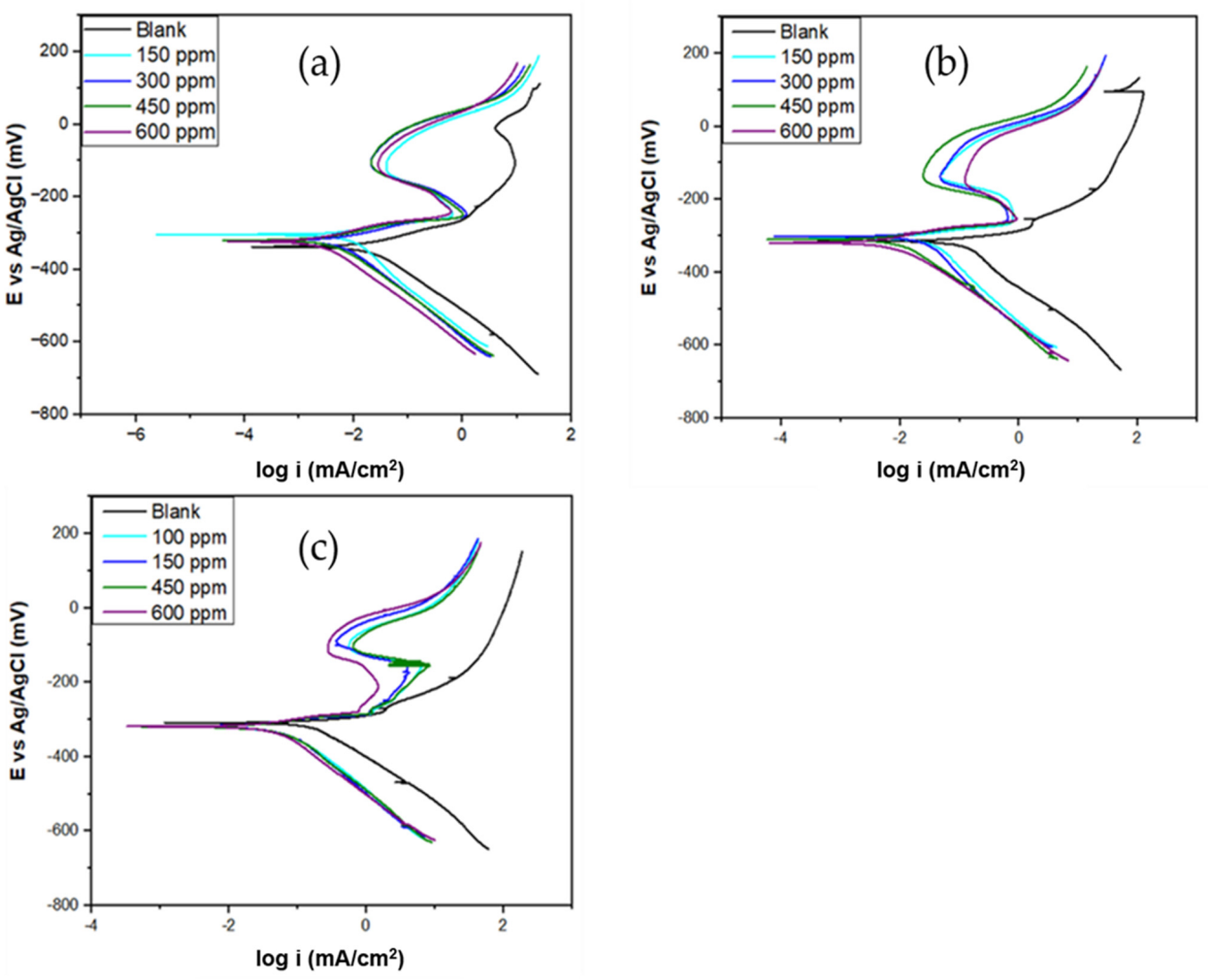

Figure 5. Polarization curves for 304 SS in 1 M HCl solution for different concentrations of *Ruta graveolens* extract at (**a**) 25 °C, (**b**) 40 °C, and (**c**) 60 °C.

Table 3. Potentiodynamic parameters for 304 SS in 1 M HCl in the absence and presence of *Ruta graveolens* at different temperatures.

Temperature (°C)	C_{inh} (ppm)	E_{corr} (−mV)	b_a (mV)	b_c (mV)	I_{corr} mA/cm^2	C_R (mm/y)	*IE*%
25	Blank	319.3	58.5	128.9	0.1302	1.595	-
	150	304.6	33.3	120.8	0.0081	0.099	94.11
	300	324.7	46.6	111.8	0.0079	0.096	94.28
	450	322.7	41.5	106.7	0.0042	0.052	97.45
	600	329	35.2	105.7	0.00302	0.037	98.10
40	Blank	299.6	49.1	133.6	0.1966	2.4083	-
	150	317.5	48.4	119.3	0.0284	0.3485	84.46
	300	306.07	47.6	120.8	0.0178	0.2185	91.87
	450	315.9	42.4	109.7	0.0142	0.1743	92.67
	600	318.5	42.5	98.1	0.0068	0.0831	96.65
60	Blank	317.3	70.2	145.8	0.3776	4.6261	-
	150	320	45.3	149.9	0.0768	0.9418	82.21
	300	319.6	44.9	140.9	0.0657	0.8057	85.56
	450	319.4	42.2	137.8	0.0588	0.7214	86.78
	600	319.1	32.6	131.7	0.0439	0.5383	90.18

The information in Figure 5 and Table 3 indicate that the E_{corr} values do not show a significant variation for the blank solution and the different inhibitor concentrations, so no specific relationship can be established between the E_{corr} and inhibitor concentration. That is, there is no significant change in the corrosion potential with increases in the extract concentration. A comparison of values of the anodic and cathodic Tafel constants for the blank and inhibitor-added solutions present different values, i.e., the anodic and cathodic branches of the polarization curves are shifted towards lower corrosion current densities, quite possibly due to a blocking effect of the adsorbed inhibitor molecules [37]. On the other hand, as shown in Table 3, increasing the inhibitor concentration decreases the value of the anodic Tafel constant, implying that *Ruta graveolens* extract facilitates the passivation of 304 stainless steel. The tendency of the anodic curves with the addition of inhibitor in all cases confirms the previously mentioned results. The anodic curve without inhibitor (blank solution) shows a quite different behavior, i.e., the curve shows an activation process (see Figure 5). In addition, the values of the cathodic Tafel constant suggest that adding an inhibitor slows the cathodic hydrogen evolution reaction. Also, it is pertinent to mention that with an increased test temperature, the corrosion current density and inhibition efficiency values decrease. Abdallah has reported a similar behavior [38]. The changes in both the anodic and cathodic slopes confirm the influence of the inhibitor on both the anodic and cathodic reactions. From the above, it seems that *R. graveolens* extract functions as a mixed-type inhibitor [39,40].

As can be observed, the corrosion rate of 304 steel in a 1 M HCl solution at 25°, 40°, and 60 °C and with an inhibitor concentration of 600 ppm decreases by more than 80%, which gives evidence of the outstanding efficiency of *Ruta graveolens* extract as an inhibitor for 304 stainless steel exposed to a 1 M HCl solution.

3.4. Electrochemical Impedance Spectroscopy

Figure 6 shows the Nyquist plots obtained from AC impedance measurements for 304 stainless steel exposed to a corrosive 1 M HCl medium in the presence of different concentrations of *Ruta graveolens* extract at 25 °C, 40 °C, and 60 °C, observing, in all cases,

the presence of a sizeable capacitive loop over the entire frequency range studied. As can be seen, the diameter of the Nyquist plots increases with an increasing extract concentration, indicating an increase in the R_{ct} values, i.e., the inhibitory film strengthens [40]. On the other hand, the maximum impedance is obtained at a concentration of 600 ppm of *Ruta Graveolens* extract. A single semicircle shows the presence of a single charge-transfer process during dissolution, which is not affected by the presence of one or a combination of inhibitory molecules [41]. At 600 ppm, the highest inhibition efficiency reached 96.32% at 25 °C, decreasing to 91.20% at 40 °C and 83.29% when the temperature was increased to 60 °C.

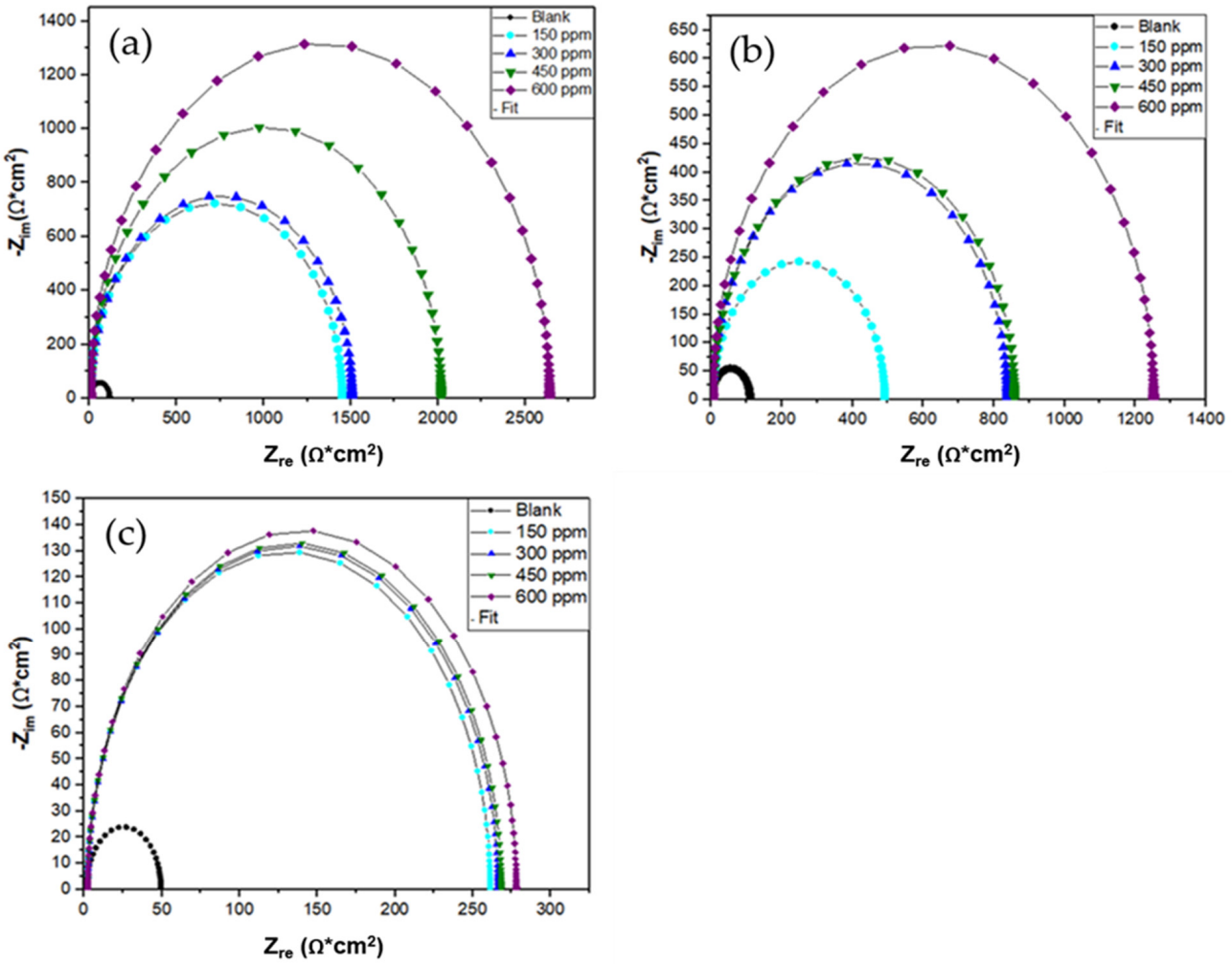

Figure 6. Nyquist plots for 304 SS in 1.0 M HCl containing 150 ppm, 300 ppm, 450 ppm, and 600 ppm of *Ruta graveolens* extract at (**a**) 25 °C, (**b**) 40 °C, and (**c**) 60 °C.

Table 4 shows the electrochemical parameters obtained from the EIS technique, such as R_s, R_{ct}, C_{dl}, I_{corr}, X^2, and $IE\%$ for 304 SS steel. These parameters were determined using the Z-View program to fit the equivalent circuit from the data obtained during the electrochemical analysis, obtaining the best fit using the Randles circuit, as shown in Figure 7. In general, this circuit corresponds to the classical parallel arrangement of the charge-transfer resistor (R_{ct}) and a constant phase element (CPE), both in series with the solution resistance (R_s).

Table 4. EIS data of 304 SS in 1 M HCl in the absence and presence of different concentrations of *Ruta graveolens* extract at various temperatures.

Temperature (°C)	Concentration	R_s (Ωcm^2)	R_{ct} (Ωcm^2)	C_{dl} ($\mu F/cm^2$)	*IE*%	X^2
25	Blank	2.01	115.2	730.0	-	0.00143
	150	3.16	1446.5	537.0	92.84	0.00147
	300	3.40	1503.6	129.0	92.48	0.00115
	450	3.99	2012.9	108.0	94.27	0.000498
	600	5.59	2635.2	59.8	96.32	0.000696
40	Blank	0.96	85.97	391.0	-	0.00553
	150	1.93	429.3	142.2	80.35	0.00647
	300	3.33	656.1	140.0	87.26	0.00218
	450	4.23	671.9	117.3	87.52	0.00643
	600	3.92	982.4	106.5	91.20	0.000477
60	Blank	1.24	37.7	430.0	-	0.00149
	150	1.50	204.2	100.4	81.25	0.00188
	300	1.94	207.7	98.6	82.47	0.00533
	450	1.76	209.5	80.4	82.36	0.00225
	600	1.82	217.1	76.5	83.29	0.000951

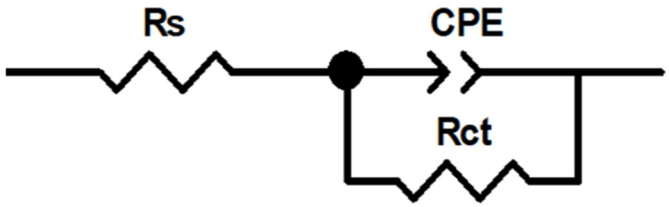

Figure 7. Randles equivalent circuit model for the *Ruta graveolens* inhibitor studied.

From Table 4, we notice that the R_{ct} values increase with an increasing extract concentration, and this implies that the charge-transfer process stops due to the adsorption of inhibitor molecules at the metal/solution interface [41].

Also, the C_{dl} value of the blank solution is higher than when in the presence of various concentrations of *Ruta graveolens* extract, which may be due to an increase in the thickness of the double layer and implies the possibility of strong adsorption of the inhibitor on the metal surface [25,42]. The Chi-squared data are lower than 10^{-3}, indicating a good fitting accuracy.

Based on the weight loss, potentiodynamic polarization, and electrochemical impedance results, the inhibitor concentration showing the highest efficiencies corresponds to 600 ppm, regardless of the test temperature.

3.5. Scanning Electron Microscopy Analysis

After stabilization of the corrosion potential, Ecorr, the time of the potentiodynamic polarization tests was about 13.33 min. The morphological characteristics obtained through SEM of the surfaces of 304 SS steel samples exposed to 1 M HCl blank solution without and with the addition of 600 ppm of *Ruta graveolens* extract at the test temperatures are shown in Figure 8. The surface morphologies of the 304 SS steel samples without addition of extract (Figure 8a,c,e) show a significantly deteriorated surface due to the corrosion of the medium. Here, the rate of deterioration is faster than the repassivation rate of the steel surface, leading to a very irregular topography. Cl- ions destroy the passive film, and the

same process of localized corrosion does not allow the repassivation of 304SS stainless steel, resulting in a continuous damage process. On the other hand, the 304 SS steel samples with the addition of *Ruta graveolens* extract, Figure 8b,d,f, show a clean surface with no evidence of corrosion damage. The adsorption of the organic compounds in the extract acts as a barrier by forming a protective surface layer, considerably decreasing the corrosion process. The above shows that *R. graveolens* extract is an excellent corrosion inhibitor for 304 SS steel.

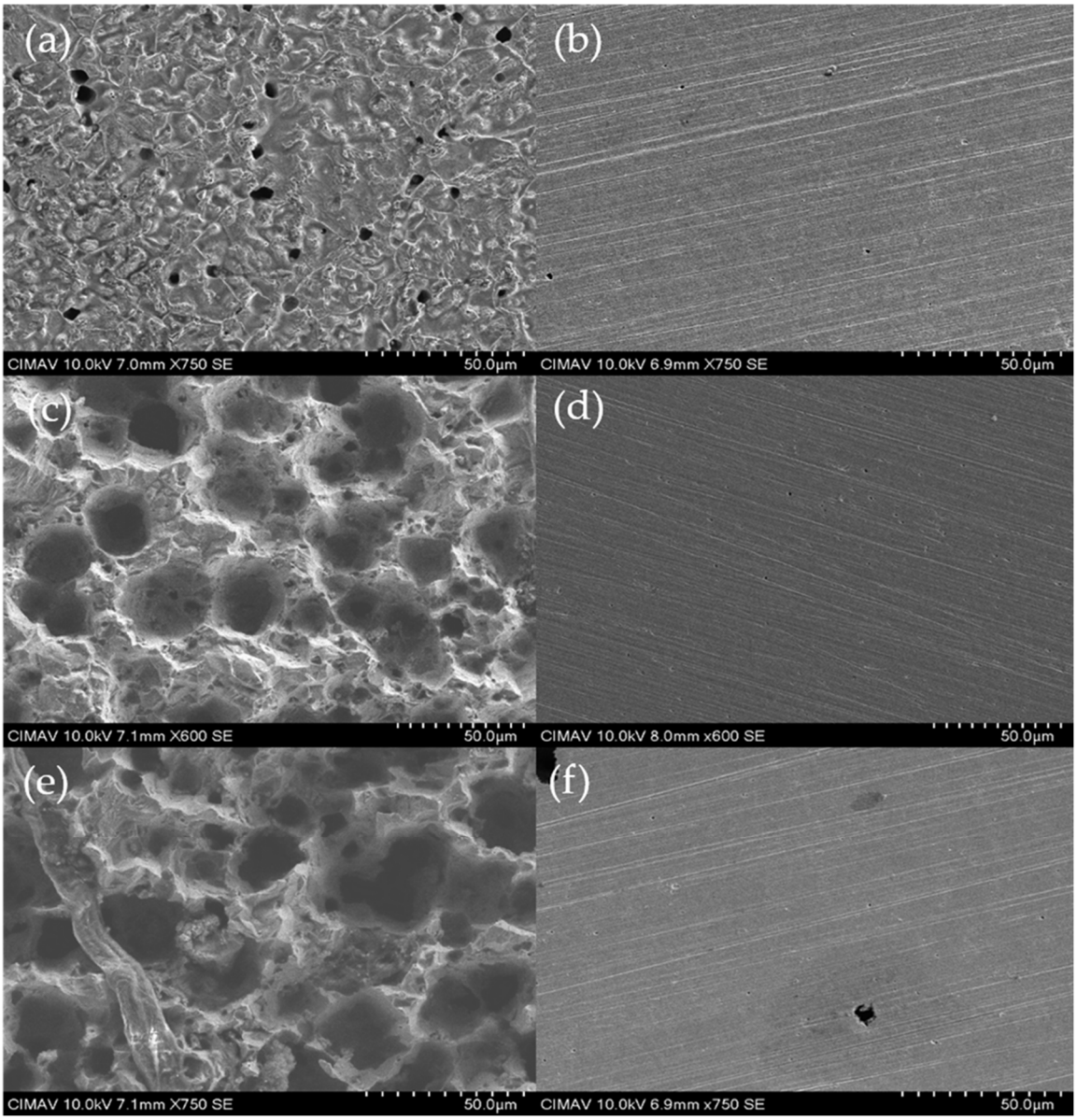

Figure 8. SEM images of samples exposed to 1 M HCl medium in the absence and presence of *Ruta graveolens* extract at a concentration of 600 ppm at 25 °C (**a**,**b**), 40 °C (**c**,**d**), and 60 °C (**e**,**f**).

3.6. Adsorption Isotherm

Adsorption isotherms are generally used to predict the nature of the interaction of molecules on the substrate surface via the adsorption mechanism. Several adsorption isotherms were calculated to describe the adsorption of *Ruta graveolens* extract on the steel surface, including Freudlich, Temkin, Frumkin, Bockris–Swinkels, Flory–Huggins, and

Langmuir isotherms. However, the one that obtained the best correlation coefficient was the Langmuir adsorption isotherm, which is represented by the following equation:

$$\frac{C}{\theta} = \frac{1}{K_{ads}} + C \tag{10}$$

where K_{ads} is the equilibrium adsorption constant, C is the extract concentration, and θ is the degree of surface coverage. Plotting concentration C versus the concentration over the fraction of surface area covered C/θ yields a linear correlation. Adsorption parameters, such as the regression coefficient R, adsorption constant (K_{ads}), Gibbs energy (ΔG), and slope values, were obtained using linear regression between C/θ and C. Figure 9 shows the different Langmuir isotherms calculated by adding varying concentrations of *Ruta graveolens* extract. Another important thermodynamic parameter is the free energy of adsorption (ΔG). The adsorption constant (K_{ads}) is related to the standard free energy of adsorption and is calculated with the following equation:

$$\Delta G = -\mathrm{RTIn}(55.5K_{ads}) \tag{11}$$

where 55.5 is the concentration of the solution water in mol/L, R is the ideal gas constant, and T is the absolute temperature. The thermodynamic parameters are summarized in Table 5. Negative values of ΔG indicate that the inhibition process of the extract on the SS 304 steel surface is spontaneous, and physisorption exists since the magnitudes of ΔG around -20 KJ/mol or lower are generated by an electrostatic interaction existing between the inhibiting extract and the metal surface charge [43–45].

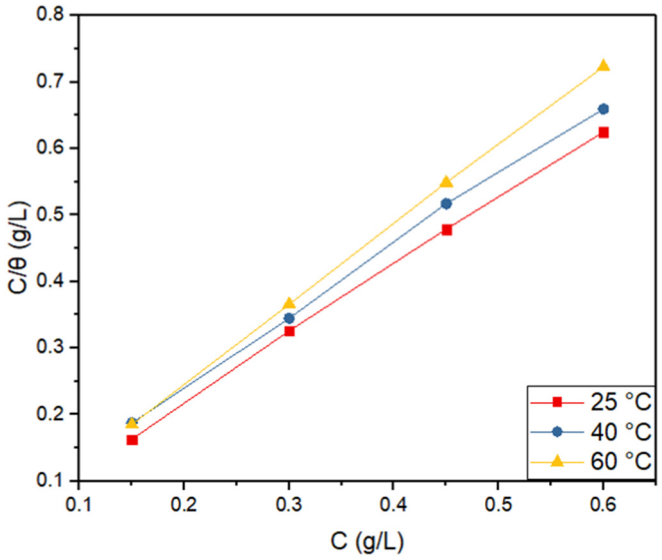

Figure 9. Langmuir adsorption plot of 304 SS in a 1 M HCl solution containing different concentrations of *Ruta graveolens*.

Table 5. Thermodynamic parameters of 304 SS steel immersed in 1 M HCl solution in the presence of *Ruta graveolens* extract.

Temperature °C	Slope	R^2	K_{ads} (KJ/mol)	ΔGads (KJ/mol)
25	1.0257	0.9994	73.5	−20.6
40	1.0586	0.9987	33	−18.6
60	1.1974	0.9999	149	−22.4

3.7. Quantum Chemical Calculations

The geometry of the molecular systems identified in the *Ruta graveolens* extract was optimized (searching for the minimum energy state) using the Gaussian 09 program and its graphical interface, GaussView 5.0 [22]. With these calculations, the geometry parameters were obtained and compared with experimental data to define the optimal methodology for performing the rest of the calculations. These parameters were calculated using different combinations of functionals and basis sets, B3LYP/6-311G (d,p), M06/6-311G (d,p), and M06-2X/6-311G (d,p). Correlation analysis showed that the best methodology used to analyze the molecular structure was B3LYP/6-311G (d,p), with an average correlation of distances and angles of 0.94. The absence of imaginary frequencies confirmed the global minima on the potential energy surface.

3.7.1. Global Chemical Activity

Figure 10 shows the images of the calculated molecules, showing their optimized structure and the mapping of HOMO and LUMO energies. The densities of these boundary orbitals in the inhibitor structures are localized and distributed around the entire molecular structure. This means that the molecules could effectively adsorb on the metallic surface.

According to the theory of boundary molecular orbitals, the electron transition is due to the interaction between the HOMO and LUMO of the reactants. One criterion to explain whether a molecule is likely to be a good corrosion inhibitor is given by the HOMO and LUMO energy values [46]. E_{HOMO} is the ability of the molecule to donate electrons. Therefore, it is related to the ionization energy (I), and high values indicate a high tendency of the molecule to donate electrons, preferably to a molecule with low energy or empty electronic orbitals. On the other hand, E_{LUMO} is related to a molecule's ability to accept electrons and is related to electron affinity (*EA*). Consequently, low *EA* values indicate a high tendency to accept electrons. The calculation of HOMO and LUMO energies is of utmost importance, since they provide relevant information about a corrosion process [47].

Thus, the probability of a molecule becoming a good inhibitor increases to the extent that it can yield electrons to metal atoms [48]. Table 6 shows the calculated values for these energies, noting key information for understanding the acceptor donor capabilities. According to the results, it can be inferred that corrosion inhibition due to HOMO energy values decreases in the following order: caffeic acid > rutin > p-coumaric acid > apigenin. Then, the inhibition efficiency of organic and inorganic compounds increases with the ability to donate electrons to the metal surface.

Table 6. Global chemical reactivity and electronic energy calculated with B3LYP/6-311G (d,p) in the solvent phase. All values are in eV.

Compound	E_{HOMO}	E_{LUMO}	ΔE	*I*	*EA*	χ	η
Rutin	−6.06	−2.04	4.02	6.03	2.10	4.16	1.97
Caffeic acid	−6.04	−2.01	4.04	6.04	2.04	4.05	2.00
p-Coumaric acid	−6.22	−1.99	4.23	6.20	2.04	4.13	2.08
Apigenin	−6.22	−2.09	4.14	6.16	2.16	4.07	4.00

The molecule's LUMO energy value indicates its ability to accept electrons [49]. The lower the energy value of this parameter, the more likely it is to accept electrons from the metal atom. Therefore, as the probability of accepting electrons increases, the molecule becomes a better corrosion inhibitor. As a result of the calculations, the values of these energies are given in Table 6. The decreasing values of LUMO energies are as follows: caffeic acid > rutin > p-coumaric acid > apigenin.

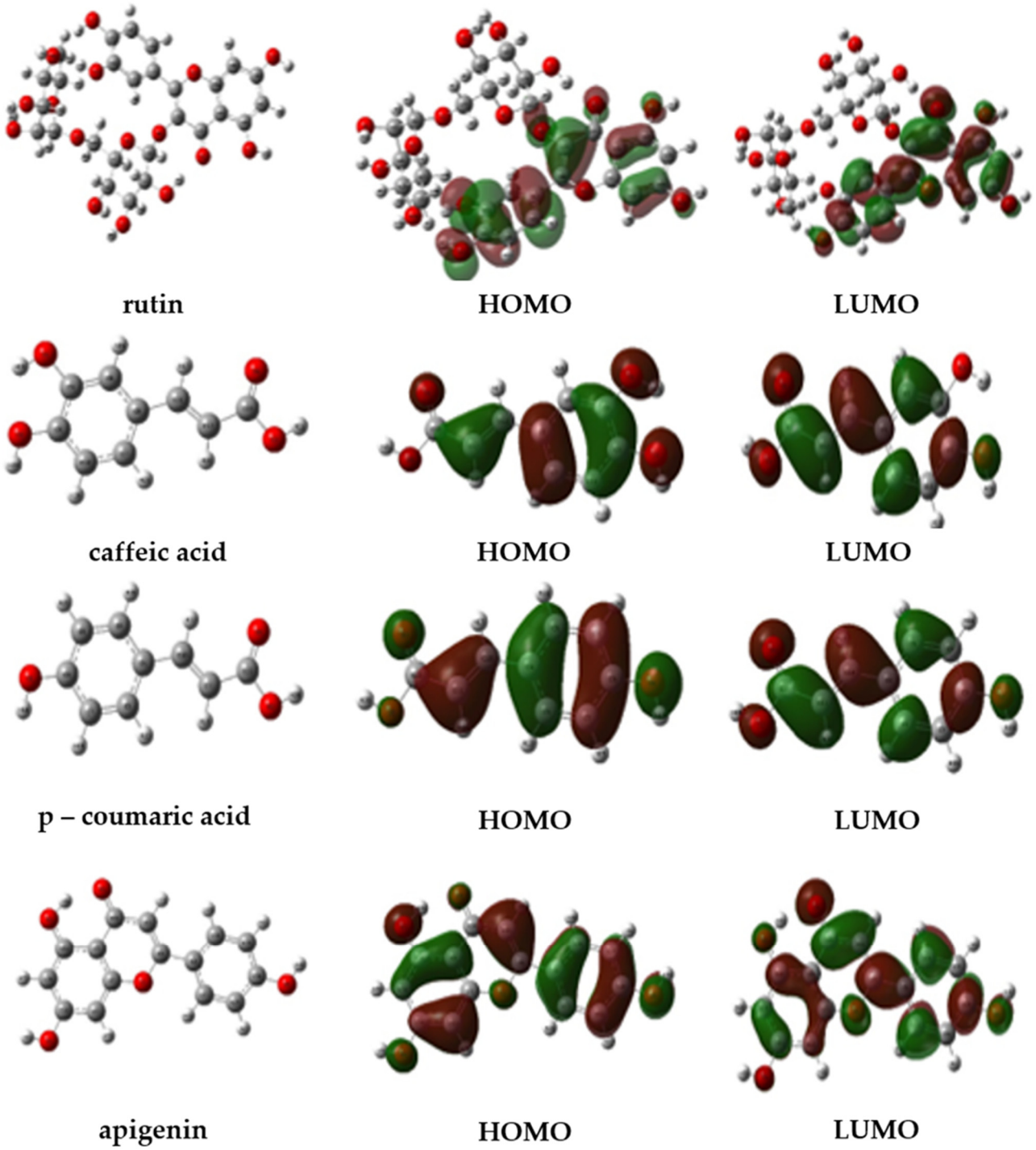

Figure 10. B3LYP/6-311G (d,p) optimized structures and HOMO and LUMO distributions for the components in *Ruta graveolens*: rutin, caffeic acid, p-coumaric acid, and apigenin.

The difference in HOMO and LUMO energies (ΔE) is an important indicator that is often associated with chemical stability [48]. This criterion is widely used to interpret and explain the intermolecular reactivity trends of inhibitor molecules. It is often associated with the ability of the molecule to donate and accept electrons from the d orbital of the metal. High values in the energy difference (ΔE) indicate high stability. In contrast, inhibitors with a small energy difference have high reactivity and, consequently, can adsorb on metal surfaces [50]. A small ΔE value is an essential requirement for corrosion inhibitors. The values calculated in descending order are p-coumaric acid > apigenin > caffeic acid > rutin.

It is observed that rutin exhibits a higher inhibition efficiency, followed by caffeic acid, apigenin, and p-coumaric.

Table 6 shows the reactivity parameters calculated according to the energy approach, which calculates the energy of the uncharged (E_N), anionic (E_{N+1}), and cationic (E_{N-1}) systems. These calculations start from the geometry of the system, which is found to be fundamental. Once the energies of the neutral and ionic states are obtained, algebraic calculations are performed to obtain the ionization potential (I), electron affinity (AE), electronegativity (χ), and chemical hardness (η). A suitable corrosion inhibitor must have a strong Lewis base [460]. The electronegativity value explains the electron transfer between the metal and the inhibitor. The results show that rutin presents a high capacity to form anions due to the electronegativity value shown in the calculation results, i.e., it shows a high tendency to attract electrons. Chemical hardness is a parameter that indicates a system's resistance to interacting with the surrounding medium. Regarding chemical hardness (η), a compound with a low hardness has a high inhibition performance, as is the case of rutin, which presented the lowest value of the compounds analyzed (see Table 6). The chemical hardness and electronegativity were used to calculate the fraction of electrons transferred.

3.7.2. Fraction of Electrons Transferred (ΔN)

Equation (6) calculated the charge transferred between phenolic acids and flavonoids (A) on the steel surface (B). The obtained values of chemical hardness (η) and electronegativity (χ) were used to determine charge transfer (ΔN), which describes the fraction of electrons transferred from system A to system B. In this case, phenolic acids were selected as system A, and type 304 stainless steel was selected as system B. Values of electronegativity (χ) and chemical hardness (η) of system B (Fe, Cr, and Ni) were obtained from the literature. If the ΔN values are positive, the system is an electron donor. If the ΔN values are negative, the system is an electron acceptor. The values obtained were positive in the interaction of the reported molecules in the *Ruta graveolens* extract and stainless steel, indicating that the charge transfer flows from the metal surface to the phenolic acids and flavonoids, respectively. This implies that the metal surface acts as an electron donor, and the phenolic-flavonoid acids act as electron acceptors. The content of the main alloying elements of steel, such as chromium and nickel, was also considered. Their values are shown in Table 7. It was observed that rutin had the highest electron transfer value, while the apigenin molecule had the lowest value, both relative to the iron atom. Concerning the chromium atom, apigenin's electron transfer was lower than rutin's. Finally, in the case of the nickel atom, there is a higher electron transfer by the rutin compared to the lower, in this case, apigenin.

Table 7. Fraction of electrons transferred (ΔN).

Molecule	ΔN_{Fe}	ΔN_{Cr}	ΔN_{Ni}
Rutin	0.746	0.039	0.033
Caffeic acid	0.737	0.032	0.032
p-Coumaric acid	0.690	0.034	0.026
Apigenin	0.355	0.031	0.016

4. Conclusions

This study reports the inhibition properties of Ruta graveolens extract as a green corrosion inhibitor for 304 stainless steel exposed to 1 M HCl medium for the first time. The extract's inhibition performance was evaluated using weight loss, potentiodynamic polarization, and electrochemical impedance techniques. The main conclusions are as follows:

- The weight loss method reveals that *Ruta graveolens* extract significantly decreases the corrosion rate of 304 steel, obtaining a maximum inhibition efficiency of 95.28%

at 25 °C and 600 ppm extract. Conversely, as the temperature and immersion time increase, the inhibition efficiency decreases.

- At 25 °C and 600 ppm extract, the potentiodynamic polarization results revealed a 98.10% inhibition efficiency. These results also indicated that the extract acted as a mixed-type inhibitor. At the same temperature and extract concentration, the electrochemical impedance results showed that the R_{ct} values increased with an increasing extract concentration, and the highest inhibition efficiency reached 96.32%.
- The adsorption of the inhibitor components onto the 304 SS surface was found to follow the Langmuir isotherm model, and the inhibition of the corrosion process is governed by physical adsorption. The thermodynamic parameters derived show negative values of standard Gibbs free adsorption energies, suggesting a spontaneous adsorption process of the *Ruta graveolens* molecules on the surface of the 304 SS.
- SEM observations prove that 304 SS's exposure to the 1 M HCl media (blank solution) causes considerable surface deterioration. On the contrary, a clean surface was observed with the addition of the inhibitor extract.
- The chemical characterization of the *Ruta graveolens* extract using HPLC showed the presence of four compounds: rutin, caffeic acid, p-coumaric acid, and apigenin. The presence of rutin molecules in the extract greatly benefits the electron donation from the HOMO of the inhibitor to the LUMO of the metal having a low ΔE value (4.02 eV).
- The present study has shown that *Ruta graveolens* extract, a green corrosion inhibitor for 304 stainless steel, has outstanding corrosion inhibition efficiency in an acidic medium.

Author Contributions: Conceptualization, J.G.C.-N., S.E.H.-S. and N.R.F.-H.; methodology, H.A.M.-R., M.S.-C. and A.D.D.; software, L.M.R.-V. and J.P.F.-D.l.R.; formal analysis, S.E.H.-S., H.A.M.-R. and J.P.F.-D.l.R.; data curation, J.G.C.-N., M.S.-C. and A.D.D.; writing—review and editing, J.G.C.-N., S.E.H.-S., N.R.F.-H. and L.M.R.-V.; project administration, J.G.C.-N. All authors have read and agreed to the published version of the manuscript.

Funding: This research received no external funding.

Data Availability Statement: The data presented in this study are available on request from the corresponding author.

Acknowledgments: SEHS acknowledges the support of CONACYT (Mexico) for providing a scholarship for her PhD studies.

Conflicts of Interest: The authors declare no conflicts of interest.

References

1. Laycock, N.J.; Newman, R.C. Localized dissolution kinetics, salt films, and pitting potentials. *Corros. Sci.* **1997**, *39*, 1771–1790. [CrossRef]
2. Leckie, H.P.; Uhlig, H.H. Environmental Factors Affecting the Critical Potential for Pitting in 18-8 Stainless Steel. *J. Electrochem. Soc.* **1966**, *113*, 1262–1267. [CrossRef]
3. Benabdellah, M.; Benkaddour, M.; Hammouti, B. Inhibition of steel corrosion in 2M H_3PO_4 by artemisia oil. *Appl. Surf. Sci.* **2006**, *252*, 6212–6217. [CrossRef]
4. Raja, P.B.; Sethuraman, M.G. Natural products as corrosion inhibitor for metals in corrosive media. *Mater. Lett.* **2008**, *62*, 113–116. [CrossRef]
5. Yilmaz, N.; Fitoz, A.; Ergun, Ü.; Emregül, K.C. A Combined Electrochemical and Theoretical Study into the Effect of 2-((thiazole-2-ylimino) methyl) phenol as a Corrosion Inhibitor for Mild Steel in a Highly Acidic Environment. *Corros. Sci.* **2016**, *111*, 110–120. [CrossRef]
6. Kertit, S.; Hammouti, B. Corrosion inhibition of iron in 1M HCl by 1-phenyl-5-mercapto-1,2,3,4-tetrazole. *Appl. Surf. Sci.* **1996**, *93*, 59–66. [CrossRef]
7. Sabu, A.S.; Ragi, K. Tinospora cordifolia extract as an environmentally benign green corrosion inhibitor in acid media: Electrochemical, surface morphological, quantum chemical, and statistical investigations. *Mater. Today Sustain.* **2021**, *13*, 100076. [CrossRef]
8. Zuo, X.; Li, W.; Luo, W.; Zhang, X.; Qiang, Y.; Zhang, J.; Li, H.; Tan, B. Research of Lilium brownii leaves extract as a commendable and green inhibitor for X70 steel, corrosion in hydrochloric acid. *J. Mol. Liq.* **2021**, *321*, 114914. [CrossRef]

9. Chapagain, A.; Acharya, D.; Das, A.K.; Chhetri, K.; Oli, H.B.; Yadav, A.P. Alkaloid of Rhynchostylis retusa as green inhibitor for mild steel corrosion in 1M H_2SO_4 solution. *Electrochem* **2022**, *3*, 211–224. [CrossRef]
10. Zaher, A.; Aslam, R.; Lee, H.-S.; Khafouri, A.; Boufellous, M.; Alrashdi, A.A.; El aoufir, Y.; Lgaz, H.; Ouhssine, M. A com-bined computational and electrochemical exploration of the Ammi visnaga L. extract as a green corrosion inhibitor for carbon steel in HCl solution. *Arab J. Chem.* **2022**, *15*, 103573. [CrossRef]
11. Tan, B.; He, J.; Zhang, S.; Xu, C.; Chen, S.; Liu, H.; Li, W. Insight into anti-corrosion nature of Betel leaves water extracts as the novel and eco-friendly inhibitors. *J. Colloid. Interface Sci.* **2021**, *585*, 287–301. [CrossRef] [PubMed]
12. de Sampaio, M.T.G.; Fernandes, C.M.; de Souza, G.G.P.; Carvalho, E.S.; Velasco, J.A.C.; Silva, J.C.M.; Alves, O.C.; Ponzio, E.A. Evaluation of aqueous extract of Mandevilla fragrans leaves as environmental-friendly corrosion inhibitor for mild steel in acid medium. *J. Bio-Tribo-Corros.* **2021**, *7*, 13–24. [CrossRef]
13. Martinez-Gonzalez, J.J.; Tello-Salgado, I.; Aviles-Flores, M.; Landeros-Martínez, L.L.; los Ríos, J.P.F.-D.; Gon-zalez-Rodriguez, J.G. Green corrosion and DFT studies of Ustilago maydis extract for carbon steel in sulfuric acid. *J. Mol. Struct.* **2023**, *1294*, 136509. [CrossRef]
14. Abdel-Gaber, A.M.; Ezzat, A.; Mohamed, M.E. Fenugreek seed and Cape gooseberry leaf extracts as green corrosion inhibitors for steel in the phosphoric acid industry. *Sci. Rep.* **2022**, *12*, 22251. [CrossRef]
15. Haque, J.; Verma, C.; Srivastava, V.; Wan Nik, W.B. Corrosion inhibition of mild steel in 1M HCl using environ-mentally benign Thevetia peruviana flower extracts. Sustain. *Chem. Pharm.* **2021**, *19*, 100354. [CrossRef]
16. Kalkhambkar, A.G.; Rajappa, S.; Manjanna, J.; Malimath, G. Saussurea obvallatta leaves extract as a potential eco-friendly corrosion inhibitor for mild steel in 1 M HCl. *Inorg. Chem. Commun.* **2022**, *143*, 109799. [CrossRef]
17. Minagalavar, R.L.; Rathod, M.R.; Rajappa, S.K.; Sajjan, A.M. Investigation of Laurus Tamala leaves extract as an environmentally acceptable corrosion inhibitor for soft steel in 1M HCl: Electrochemical, DFT, and surface characterization techniques. *Indian J. Chem. Technol.* **2023**, *30*, 492–505. [CrossRef]
18. Pai, G.D.; Rathod, M.R.; Rajappa, S.K.; Kittur, A.A. Effect of tabebuia heterophylla plant leaves extract on corrosion protection of low carbon steel in 1M HCl medium: Electrochemical, quantum chemical and surface characterization studies. *Results Surf. Interfaces* **2024**, *15*, 100203. [CrossRef]
19. Fouda, E.-A.; El-Hossiany, A.; Ramadan, H. Calotropis Procera plant extract as green corrosion inhibitor for 304 stainless steel in hydrochloric acid solution. *Zast. Mater.* **2018**, *58*, 541–555. [CrossRef]
20. Ehsani, A.; Mahjani, M.G.; Hosseini, M.; Safari, R.; Moshrefi, R.; Shiri, H.M. Evaluation of Thymus vulgaris plant extract as an eco-friendly corrosion inhibitor for stainless steel 304 in acidic solution by means of electrochemical impedance spectroscopy, electrochemical noise analysis and density functional theory. *J. Colloid Interface Sci.* **2016**, *490*, 444–451. [CrossRef]
21. Albrimi, Y.A.; Addi, A.A.; Douch, J.; Hamdani, M.; Souto, R.M. Studies on the adsorption of heptamolybdate ions on AISI 304 stainless steel from acidic HCl solution for corrosion inhibition. *Int. J. Electrochem. Sci.* **2016**, *11*, 385–397. [CrossRef]
22. Fouda, A.S.; Shalabi, K.; Shohba, R.M.A. Chalcones as Environmentally-Friendly Corrosion Inhibitors for Stainless Steel Type 304 in 1 M HCl Solutions. *Int. J. Electrochem. Sci.* **2014**, *9*, 9876–9893. [CrossRef]
23. Soltani, N.; Tavakkoli, N.; Kashani, M.K.; Mosavizadeh, A.; Oguzie, E.E.; Jalali, M.R. Silybum marianum extract as a natural source inhibitor for 304 stainless steel corrosion in 1.0M HCl. *J. Ind. Eng. Chem.* **2014**, *20*, 3217–3227. [CrossRef]
24. Scendo, M.; Trela, J. Adenine as an effective corrosion inhibitor for stainless steel in chloride solution. *Int. J. Electrochem. Sci.* **2013**, *8*, 9201–9221. [CrossRef]
25. Soltani, N.; Tavakkoli, N.; Khayatkashani, M.; Jalali, M.R.; Mosavizade, A. Green approach to corrosion inhibition of 304 stainless steel in hydrochloric acid solution by the extract of Salvia officinalis leaves. *Corros. Sci.* **2012**, *62*, 122–135. [CrossRef]
26. Asgharian, S.; Hojjati, M.R.; Ahrari, M.; Bijad, E.; Deris, F.; Lorigooini, Z. Ruta graveolens and rutin, as its major compound: Investigating their effect on spatial memory and passive avoidance memory in rats. *Pharm. Biol.* **2020**, *58*, 447–453. [CrossRef]
27. Manssouri, M.; Chraka, A.; Raissouni, I.; Wahby, A. Anti-Corrosion Performance of Ruta Graveolens Essential Oil as A Green Inhibitor for Mild Steel in 1 M HCl: Evaluations of Electrochemical, DFT and Monte Carlo. *Anal. Bioanal. Electrochem.* **2024**, *16*, 507–536. [CrossRef]
28. Anupama, K.K.; Shainy, K.M.; Joseph, A. Excellent Anticorrosion Behavior of Ruta Graveolens Extract (RGE) for Mild Steel in Hydrochloric Acid: Electro Analytical Studies on the Effect of Time, Temperature, and Inhibitor Concentration. *J. Bio-Tribo-Corros.* **2016**, *2*, article no. 2. [CrossRef]
29. Alao, A.O.; Popoola, A.P.; Dada, M.O.; Sanni, O. Utilization of green inhibitors as a sustainable corrosion control method for steel in petrochemical industries: A review. *Front. Energy Res.* **2023**, *10*, 1063315. [CrossRef]
30. Li, P.; Tanb, J.Y.L.K.L.; Leea, J.Y. Electrochemical impedance and X-ray photoelectron spectroscopic studies of the inhibition of mild steel corrosion in acids by cyclohexylamine. *Electrochim. Acta* **1997**, *42*, 605–615. [CrossRef]
31. *ASTM G3-14(2019)*; Standard Practice for Conventions Applicable to Electrochemical Measurements. ASTM International: West Conshohocken, PA, USA, 2019.
32. Frisch, M.J.; Trucks, G.W.; Schlegel, H.B.; Scuseria, G.E.; Robb, M.A.; Cheeseman, J.R.; Scalmani, G.; Barone, V.; Petersson, G.A.; Nakatsuji, H.; et al. *Gaussian 09, Revision A.02*; Gaussian, Inc.: Wallingford, CT, USA, 2009.
33. Becke, A.D. Densityfunctional thermochemistry IV. A new dynamical correlation functional and implications for exact-exchange mixing functional and implications for exact-exchange mixing. *J. Chem. Phys.* **1996**, *104*, 1040–1046. [CrossRef]
34. Becke, A.D.; Johnson, E.R. A density-functional model of the dispersion interaction. *J. Chem. Phys.* **2014**, *123*, 154101. [CrossRef]

35. Becke, A.D. A new mixing of Hartree–Fock and local density-functional theories. *J. Chem. Phys.* **1993**, *98*, 1372–1377. [CrossRef]
36. Zhao, Y.; Truhlar, D.G. The M06 suite of density functionals for main group thermochemistry, thermochemical kinetics, noncovalent interactions, excited states, and transition elements: Two new functionals and systematic testing of four M06-class functionals and 12 other functions. *Theor. Chem. Acc.* **2008**, *120*, 215–241. [CrossRef]
37. Alvarez, P.E.; Fiori-Bimbi, M.V.; Neske, A.; Brandán, S.A.; Gervasi, C.A. Rollinia occidentalis extract as green corrosion inhibitor for carbon steel in HCl solution. *J. Ind. Eng. Chem.* **2018**, *58*, 92–99. [CrossRef]
38. Abdallah, M. Rhodanine azosulpha drugs as corrosion inhibitors for corrosion of 304 stainless steel in hydrochloric acid solution. *Corros. Sci.* **2002**, *44*, 717–728. [CrossRef]
39. Kowsari, E.; Arman, S.; Shahini, M.; Zandi, H.; Ehsani, A.; Naderi, R.; PourghasemiHanza, A.; Mehdipour, M. In situ synthesis, electrochemical and quantum chemical analysis of an amino acid-derived ionic liquid inhibitor for corrosion protection of mild steel in 1M HCl solution. *Corros. Sci.* **2016**, *112*, 73–85. [CrossRef]
40. Joseph, A.; Joseph, A. Surface Interaction and Corrosion Inhibition of Mild Steel in Hydrochloric Acid Using Pyoverdine, an Eco-Friendly Bio-molecule. *J. Bio-Tribo-Corros.* **2016**, *2*, 20. [CrossRef]
41. Bhardwaj, N.; Sharma, P.; Guo, L.; Dagdag, O.; Kumar, V. Molecular dynamic simulation, quantum chemical calculation and friendly corrosion inhibitor for stainless steel (SS-410) in acidic medium. *J. Mol. Liq.* **2022**, *346*, 118237. [CrossRef]
42. Behpour, M.; Ghoreishi, S.M.; Soltani, N. The inhibitive effect of some bis-N, S-bidentate Schiff bases on corrosion behavior of 304 stainless steel in hydrochloric acid solution. *Corros. Sci.* **2009**, *51*, 1073–1082. [CrossRef]
43. Hussin, M.H.; Abdul, A.; Nasir, M.; Ibrahim, M.; Brosse, N. The capability of ultrafiltrated alkaline and organosolv oil palm (*Elaeis guineensis*) fronds lignin as green corrosion inhibitor for mild steel in 0.5 M HCl solution. *Measurement* **2016**, *78*, 90–103. [CrossRef]
44. Gapsari, F.; Soenoko, R.; Suprapto, A.; Suprapto, W. Bee Wax Propolis Extract as Eco-Friendly Corrosion Inhibitors for 304SS in Sulfuric Acid. *Int. J. Corros.* **2015**, *2015*, 567202. [CrossRef]
45. Gapsari, F.; Madurani, K.A.; Simanjuntak, F.M. Corrosion Inhibition of Honeycomb Waste Extracts for 304 Stainless Steel in Sulfuric Acid Solution. *Materials* **2019**, *12*, 2120. [CrossRef]
46. Tu, B. Quantum chemical study of thiaozole derivatives as corrosion inhibitors based on density functional theory. *Arab. J. Chem.* **2021**, *14*, 102927. [CrossRef]
47. Kokalj, A. On the alleged importance of the molecular electron-donating ability and the HOMO-LUMO gap in corrosion inhibition studies. *Corros. Sci.* **2020**, *180*, 109016. [CrossRef]
48. Kaya, S.; Burak, T.; Kaya, C.; Obot, I.B. Determination of corrosion inhibition effects of amino acids: Quantum chemical and molecular dynamic simulation study. *J. Taiwan Inst. Chem. Eng.* **2015**, *58*, 528–535. [CrossRef]
49. Bhawsar, J.; Jain, P.; Rani, M. Quantum Chemical Assessment of Two Natural Compounds: Vasicine and Vasicinone as Green Corrosion Inhibitors. *Int. J. Electrochem. Sci.* **2018**, *13*, 3200–3209. [CrossRef]
50. Ammouchi, N.; Allal, H.; Belhocine, Y.; Bettaz, S.; Zouaoui, E. DFT computations, and molecular dynamics investigations on conformers of some pyrazinamide derivatives as corrosion inhibitors for aluminum. *J. Mol. Liq.* **2020**, *300*, 112309. [CrossRef]